

On the Outage Probability of Vehicular Communications at Intersections Over Nakagami- m Fading Channels

Baha Eddine Youcef Belmekki¹, Abdelkrim Hamza², and Benoît Escrig¹

¹IRIT Laboratory, School of ENSEEIHT, Institut National Polytechnique de Toulouse, France,
e-mail: {bahaeddine.belmekki, benoit.escrig}@enseeiht.fr

²LISIC Laboratory, Electronic and Computer Faculty, USTHB, Algiers, Algeria,
email: ahamza@usthb.dz

Abstract

In this paper, we study vehicular communications (VCs) at intersections, in the presence of interference over Nakagami- m fading channels. The interference are originated from vehicles located on two perpendicular roads. We derive the outage probability, and closed forms are obtained. The outage probability is derived when the destination is on the road (vehicle, cyclist, pedestrian) or outside the road (base station, road side unit). We compare the performance of line of sight (LOS) scenarios and non-line of sight (NLOS) scenarios, and show that NLOS scenarios offer better performance than LOS scenarios. We also compare intersection scenarios with highway scenarios, and show that the performance of intersection scenarios are worst than highway scenarios as the destination moves toward the intersection. Finally, we investigate the performance of VCs in a realistic scenario involving several lanes. All the analytical results are validated by Monte-Carlo simulations.

Index Terms

Vehicular communications, interference, outage probability, throughput, stochastic geometry, intersections.

I. INTRODUCTION

A. Motivation

Road traffic safety is a major issue, and more particularly at intersections [1]. Vehicular communications (VCs) offer several applications regarding accident prevention, such as sending

safety messages that alert vehicles about accidents happening in their surrounding. One of the major drawbacks that effect VCs are interference. Hence, investigating the performance of VCs in the presence of interference is crucial in order to design safety applications at urban and suburban intersections.

B. Related Works

The impact of the presence of interference in VCs considering highway scenarios has been investigated in [2]–[4]. In [5], the authors derive the expressions for the intensity of concurrent transmitters and packet success probability in multi-lane highways with carrier sense multiple access (CSMA) protocols. The performance of IEEE 802.11p using tools from queuing theory and stochastic geometry is analyzed in [6]. The authors in [7] derivate the outage probability and rate coverage probability of vehicles, when the line of sight (LOS) path to the base station is obstructed by large vehicles sharing other highway lanes. In [8], the performance of automotive radar is evaluated in terms of expected signal-to-noise ratio, when the locations of vehicles follow a Poisson point process and a Bernoulli lattice process.

However, few works studied the effect of interference in VCs at intersections. Steinmetz et al derivate the success probability when the received node and the interferer nodes are aligned on the road [9]. In [10], the authors analyze the performance in terms of success probability for finite road segments under different channel conditions. The authors in [11] evaluate the average and the fine-grained reliability for interference-limited vehicle-to-vehicle (V2V) communications with the use of the meta distribution. In [12], the authors analyze the performance of an orthogonal street system which consists of multiple intersections, and show that, in high-reliability regime, the orthogonal street system behaves like a one dimensional Poisson network. However, in low-reliability regime, it behaves like a two dimensional Poisson network. The authors in [13] derive the outage probability of V2V communications at intersections in the presence of interference with a power control strategy.

The authors of this the paper investigated the impact of NOMA using direct transmission in [14], [15], cooperative NOMA at intersections in [16], [17], and MRC using NOMA [18], and in millimeter wave vehicular communications in [19], [20]. The authors of this paper also investigated the impact of vehicles mobility, and different transmission schemes on the performance in [21] and [22], respectively.

Following this line of research, we study the performance of VCs at urban and suburban intersections in the presence of interference.

C. Contributions

The contributions of this paper are as follows:

- We derived the outage probability expressions over Nakagami- m fading channels for specific channel conditions, and when the destination is either on the road (V2V) or outside the road (V2I).
- We compare the performance of suburban (LOS) environment and urban (NLOS) environment, and show that, the urban environment exhibits better performance than suburban environment.
- We compare intersection scenarios with highway scenarios, and show that the performance of intersection scenarios are worst than highway scenarios as the destination moves toward the intersection.
- We investigate a realistic scenario involving several lanes, and show that the increase of lanes decreases the performance.

II. SYSTEM MODEL

In this paper, we consider a transmission between a source, denoted S , and a destination, denoted D . We denote by S and D the nodes and their locations. We consider an intersection scenario with two perpendicular roads, an horizontal road denoted X , and a vertical road denoted Y . In this paper, we consider both V2V and V2I communications, hence, S and D can be either on the road (e.g., vehicle) or outside the road (e.g., base station). We denote by d the distance between D and the intersection as shown in Fig.1. Note that the intersection is the point where the X road and the Y road intersect.

The transmission is subject to interference originated from vehicles located on the roads. The set of interfering vehicles located on the X road, denoted by Φ_X (resp. on the Y road, denoted by Φ_Y) are modeled as a One-Dimensional Homogeneous Poisson Point Process (1D-HPPP), that is, $\Phi_X \sim 1D\text{-HPPP}(\lambda_X, x)$ (resp. $\Phi_Y \sim 1D\text{-HPPP}(\lambda_Y, y)$), where x and λ_X (resp. y and λ_Y) are the position of interferer vehicles and their intensity on the X road (resp. Y road). The notation x and y denotes both the interfering vehicles and their locations.

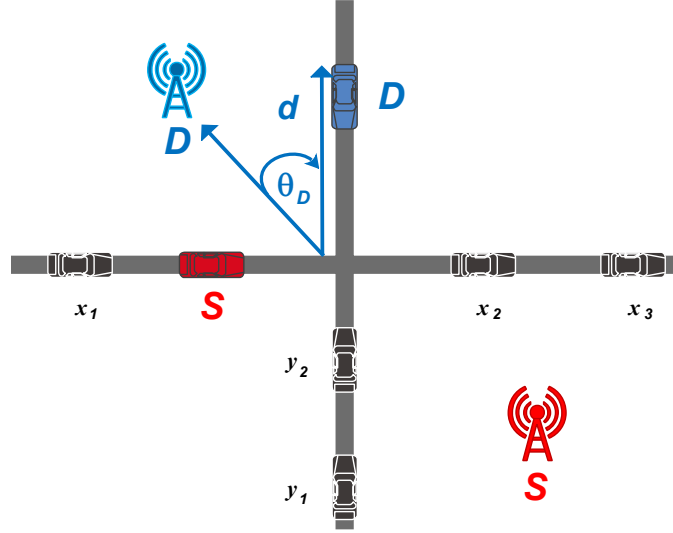


Fig. 1: System model for VCs at the intersection. The nodes S and D can either be vehicles or as part of communication infrastructures.

The medium access protocols used in VCs are mainly based on CSMA schemes. However, the mathematical derivation considering these protocols might not be possible in our scenario, and closed form expressions are hard to obtain. In addition, [23], [24] showed that the performance of CSMA tends to the performance of ALOHA in dense networks. Hence, we assume that vehicles use slotted Aloha MAC protocol with parameter p , i.e., every node can access the medium with a probability p

The transmission between the nodes a and b experiences a path loss denoted by l_{ab} , where $l_{ab} = \|a - b\|^{-\alpha}$, and α is the path loss exponent.

We consider an interference limited scenario, hence, the power of noise is set to zero ($\sigma^2 = 0$). Without loss of generality, we assume that all nodes transmit with a unit power. The signal received at D is expressed as

$$\mathcal{Y}_D = h_{SD}\sqrt{l_{SD}}\chi_S + \sum_{x \in \Phi_X} h_{Dx}\sqrt{l_{Dx}}\chi_x + \sum_{y \in \Phi_Y} h_{Dy}\sqrt{l_{Dy}}\chi_y,$$

where \mathcal{Y}_D is the signal received by D . The messages transmitted by the interfere node x and y , are denoted respectively by χ_x and χ_y , h_{SD} denotes the fading coefficient between S and D , and it is modeled as Nakagami- m fading with parameter m [25]. Therefore, the power fading coefficient between the node S and D , denoted $|h_{SD}|^2$, follows a gamma distribution distribution.

The aggregate interference is defined as

$$I_X = \sum_{x \in \Phi_X} |h_{Dx}|^2 l_{Dx} \quad (1)$$

$$I_Y = \sum_{y \in \Phi_Y} |h_{Dy}|^2 l_{Dy}, \quad (2)$$

where I_X denotes the aggregate interference from the X road, I_Y denotes the aggregate interference from the Y , Φ_X denotes the set of the interferers from the X road, and Φ_Y denotes the set of the interferers from the Y road. The coefficients h_{Dx} and h_{Dy} denote the fading between D and x , and between D and y respectively. They are modeled as Rayleigh fading [26]. Then, the power fading coefficients $|h_{Dx}|^2$ and $|h_{Dy}|^2$, follow an exponential distribution with unit mean.

We consider two scenarios, the LOS scenario, and the non-line of sight scenario (NLOS). The LOS scenario models the suburban environment, whereas the NLOS scenario models the urban scenario. We denote by α_{LOS} and m_{LOS} , the path exponent and the fading parameter for LOS, and we denote by α_{NLOS} and m_{NLOS} the path exponent and the fading parameter for NLOS. Hence, we have that $m \in \{m_{\text{LOS}}, m_{\text{NLOS}}\}$ $\alpha \in \{\alpha_{\text{LOS}}, \alpha_{\text{NLOS}}\}$.

III. OUTAGE EXPRESSIONS

In this section, we calculate the outage probability of the transmission between S and D . An outage event occurs when the SIR at D is below a given threshold. The SIR at D is defined as

$$\text{SIR} \triangleq \frac{|h_{SD}|^2 l_{SD}}{I_X + I_Y}. \quad (3)$$

The outage event at D is defined as

$$O \triangleq \left[\text{SIR} < \Theta \right], \quad (4)$$

where Θ is the decoding threshold. The outage probability expression is given as

$$\mathbb{P}(O) = \mathbb{P}(\text{SIR} < \Theta) = 1 - \mathbb{P}(\text{SIR} \geq \Theta). \quad (5)$$

To calculate $\mathbb{P}(\text{SIR} \geq \Theta)$, we proceed as follows

$$\begin{aligned} \mathbb{P}(\text{SIR} \geq \Theta) &= \mathbb{E}_{I_X, I_Y} \left[\mathbb{P} \left\{ \frac{|h_{SD}|^2 l_{SD}}{I_X + I_Y} \geq \Theta \right\} \right] \\ &= \mathbb{E}_{I_X, I_Y} \left[\mathbb{P} \left\{ |h_{SD}|^2 \geq \frac{\Theta}{l_{SD}} (I_X + I_Y) \right\} \right]. \end{aligned} \quad (6)$$

Since $|h_{SD}|^2$ follows a gamma distribution, its complementary cumulative distribution function (CCDF) is given by

$$\bar{F}_{|h_{SD}|^2}(X) = \mathbb{P}(|h_{SD}|^2 > X) = \frac{\Gamma(m, \frac{m}{\mu}X)}{\Gamma(m)}, \quad (7)$$

hence

$$\mathbb{P}(\text{SIR} \geq \Theta) = \mathbb{E}_{I_X, I_Y} \left[\frac{\Gamma\left(m, \frac{m\Theta}{\mu l_{SD}}(I_X + I_Y)\right)}{\Gamma(m)} \right]. \quad (8)$$

The exponential sum function when m is an integer is defined as

$$e_{(m)} = \sum_{k=0}^{m-1} \frac{\left(\frac{m}{\mu}X\right)^k}{k!} = e^x \frac{\Gamma(m, \frac{m}{\mu}X)}{\Gamma(m)}, \quad (9)$$

then

$$\frac{\Gamma(m, \frac{m}{\mu}X)}{\Gamma(m)} = e^{-\frac{m}{\mu}X} \sum_{k=0}^{m-1} \frac{1}{k!} \left(\frac{m}{\mu}X\right)^k. \quad (10)$$

The equation (8) then becomes

$$\mathbb{P}(\text{SIR} \geq \Theta) = \sum_{k=0}^{m-1} \frac{1}{k!} \left(\frac{m\Theta}{\mu l_{SD}}\right)^k \mathbb{E}_{I_X, I_Y} \left[\exp\left(-\frac{m\Theta}{\mu l_{SD}}(I_X + I_Y)\right) (I_X + I_Y)^k \right]. \quad (11)$$

Applying the binomial theorem in (11), we get

$$\mathbb{P}(\text{SIR} \geq \Theta) = \sum_{k=0}^{m-1} \frac{1}{k!} G^k \mathbb{E}_{I_X, I_Y} \left[\exp\left(-G[I_X + I_Y]\right) \sum_{n=0}^k \binom{k}{n} I_X^{k-n} I_Y^n \right], \quad (12)$$

where $G = \frac{m\Theta}{\mu l_{SD}}$. We denote, by $\mathcal{A}(I_X, I_Y)$, the expectation in (12), hence $\mathcal{A}(I_X, I_Y)$ becomes

$$\begin{aligned} \mathcal{A}(I_X, I_Y) &= \mathbb{E}_{I_X, I_Y} \left[e^{-G I_X} e^{-G I_Y} \sum_{n=0}^k \binom{k}{n} I_X^{k-n} I_Y^n \right] \\ &= \sum_{n=0}^k \binom{k}{n} \mathbb{E}_{I_X, I_Y} \left[e^{-G I_X} e^{-G I_Y} I_X^{k-n} I_Y^n \right] \\ &= \sum_{n=0}^k \binom{k}{n} \mathbb{E}_{I_X} \left[e^{-G I_X} I_X^{k-n} \right] \mathbb{E}_{I_Y} \left[e^{-G I_Y} I_Y^n \right] \\ &= \sum_{n=0}^k \binom{k}{n} (-1)^{k-n} \frac{d^{k-n} \mathcal{L}_{I_X}(G)}{d^{k-n} G} (-1)^n \frac{d^n \mathcal{L}_{I_Y}(G)}{d^n G} \\ &= (-1)^k \sum_{n=0}^k \binom{k}{n} \frac{d^{k-n} \mathcal{L}_{I_X}(G)}{d^{k-n} G} \frac{d^n \mathcal{L}_{I_Y}(G)}{d^n G}. \end{aligned} \quad (13)$$

Using the following property

$$\mathbb{E}_I \left[e^{-gI} I^N \right] = (-1)^N \frac{d^N \mathbb{E}_I \left[e^{-gI} I^N \right]}{d^N g} = (-1)^N \frac{d^N \mathcal{L}_I(g)}{d^N g}, \quad (14)$$

then

$$\mathbb{P}(\text{SIR} \geq \Theta) = \sum_{k=0}^{m-1} \frac{1}{k!} \left(-\frac{m\Theta}{\mu l_{SD}} \right)^k \sum_{n=0}^k \binom{k}{n} \frac{d^{k-n} \mathcal{L}_{I_X} \left(\frac{m\Theta}{\mu l_{SD}} \right) d^n \mathcal{L}_{I_Y} \left(\frac{m\Theta}{\mu l_{SD}} \right)}{d^{k-n} \left(\frac{m\Theta}{\mu l_{SD}} \right) d^n \left(\frac{m\Theta}{\mu l_{SD}} \right)}. \quad (15)$$

Plugging (15) into (5) yields of the outage probability expression. The expression of $d^{k-n} \mathcal{L}_{I_X}(s)/d^{k-n}(s)$ and $d^n \mathcal{L}_{I_Y}(s)/d^n(s)$ are given respectively by

$$\begin{aligned} \frac{d^n \mathcal{L}_{I_{X_D}}(s)}{d^n s} &= \left[-\frac{1}{4} \frac{p\lambda_Y \pi (\sqrt{d_y^4 + s} - d_y^2)}{\sqrt{2\sqrt{d_y^4 + s} + 2d_y^2(d_y^4 + s)}} \right. \\ &\quad \left. -\frac{1}{4} \frac{p\lambda_Y \pi \sqrt{2\sqrt{d_y^4 + s} + 2d_y^2}}{d_y^4 + s} + \frac{1}{4} \frac{p\lambda_Y \pi \sqrt{2\sqrt{d_y^4 + s} + 2d_y^2} (\sqrt{d_y^4 + s} - d_y^2)}{(d_y^4 + s)^{3/2}} \right]^n \\ &\quad \times \exp \left(-\frac{1}{2} \frac{p\lambda_Y \pi \sqrt{2\sqrt{d_y^4 + s} + 2d_y^2} (\sqrt{d_y^4 + s} - d_y^2)}{\sqrt{d_y^4 + s}} \right), \end{aligned} \quad (16)$$

and

$$\begin{aligned} \frac{d^n \mathcal{L}_{I_{Y_D}}(s)}{d^n s} &= \left[-\frac{1}{4} \frac{p\lambda_Y \pi (\sqrt{d_x^4 + s} - d_x^2)}{\sqrt{2\sqrt{d_x^4 + s} + 2d_x^2(d_x^4 + s)}} \right. \\ &\quad \left. -\frac{1}{4} \frac{p\lambda_Y \pi \sqrt{2\sqrt{d_x^4 + s} + 2d_x^2}}{d_x^4 + s} + \frac{1}{4} \frac{p\lambda_Y \pi \sqrt{2\sqrt{d_x^4 + s} + 2d_x^2} (\sqrt{d_x^4 + s} - d_x^2)}{(d_x^4 + s)^{3/2}} \right]^n \\ &\quad \times \exp \left(-\frac{1}{2} \frac{p\lambda_Y \pi \sqrt{2\sqrt{d_x^4 + s} + 2d_x^2} (\sqrt{d_x^4 + s} - d_x^2)}{\sqrt{d_x^4 + s}} \right). \end{aligned} \quad (17)$$

IV. LAPLACE TRANSFORM EXPRESSIONS

After we obtained the expression of the outage probability, we derive, in this section, the Laplace transform expressions of the interference from the X road and from the Y road. The Laplace transform of the interference originating from the X road, is expressed as

$$\mathcal{L}_{I_X}(s) = \mathbb{E} \left[\exp(-sI_X) \right]. \quad (18)$$

Plugging (1) into (18) yields

$$\begin{aligned} \mathcal{L}_{I_X}(s) &= \mathbb{E} \left[\exp \left(- \sum_{x \in \Phi_X} s |h_{D_x}|^2 l_{D_x} \right) \right] \\ &= \mathbb{E} \left[\prod_{x \in \Phi_X} \exp \left(- s |h_{D_x}|^2 l_{D_x} \right) \right] \\ &\stackrel{(a)}{=} \mathbb{E} \left[\prod_{x \in \Phi_X} \mathbb{E}_{|h_{D_x}|^2, p} \left\{ \exp \left(- s |h_{D_x}|^2 l_{D_x} \right) \right\} \right] \\ &\stackrel{(b)}{=} \mathbb{E} \left[\prod_{x \in \Phi_X} \frac{p}{1 + s l_{D_x}} + 1 - p \right] \\ &\stackrel{(c)}{=} \exp \left(- \lambda_X \int_{\mathbb{R}} \left[1 - \left(\frac{p}{1 + s l_{D_x}} + 1 - p \right) \right] dx \right) \\ &= \exp \left(- p \lambda_X \int_{\mathbb{R}} \frac{1}{1 + 1/s l_{D_x}} dx \right), \end{aligned} \quad (19)$$

where (a) follows from the independence of the fading coefficients; (b) follows from performing the expectation over $|h_{D_x}|^2$ which follows an exponential distribution with unit mean, and performing the expectation over the set of interferers; (c) follows from the probability generating functional (PGFL) of a PPP [27]. Then, substituting $l_{D_x} = \|x - D\|^{-\alpha}$ in (19) yields

$$\mathcal{L}_{I_X}(s) = \exp \left(- p \lambda_X \int_{\mathbb{R}} \frac{1}{1 + \|x - D\|^\alpha / s} dx \right), \quad (20)$$

where

$$\|x - D\| = \sqrt{\left[d \sin(\theta_D) \right]^2 + \left[x - d \cos(\theta_D) \right]^2}. \quad (21)$$

The Laplace transform of the interference originating from the Y road can be acquired by following the same steps above, and it is given by

$$\mathcal{L}_{I_Y}(s) = \exp \left(- p \lambda_Y \int_{\mathbb{R}} \frac{1}{1 + \|y - D\|^\alpha / s} dy \right), \quad (22)$$

where

$$\|y - D\| = \sqrt{\left[d \cos(\theta_D)\right]^2 + \left[y - d \sin(\theta_D)\right]^2}, \quad (23)$$

where θ_D is the angle between the node D and the X road.

The expression (20) and (22) can be calculated with mathematical tools such as MATLAB. Closed form expressions are obtained for $\alpha = 2$ and $\alpha = 4$. We only present the expressions when $\alpha = 4$ due to lack of space.

In order to calculate the Laplace transform of interference originated from the X road at D , we have to calculate the integral in (20) for $\alpha = 4$. Let us take $d_x = d \cos(\theta_D)$, and $d_y = d \sin(\theta_D)$, then (20) becomes

$$\begin{aligned} \mathcal{L}_{I_{X_D}}(s) &= \\ &= \exp\left(-p\lambda_X \int_{\mathbb{R}} \frac{1}{1 + \left(\sqrt{d_y^2 + (x - d_x)^2}\right)^4 / s} dx\right) \\ &= \exp\left(-p\lambda_X s \int_{\mathbb{R}} \frac{1}{s + \left(\sqrt{d_y^2 + (x - d_x)^2}\right)^4} dx\right), \end{aligned} \quad (24)$$

and the integral inside the exponential in (24) equals

$$\int_{\mathbb{R}} \frac{1}{s + \left(\sqrt{d_y^2 + (x - d_x)^2}\right)^4} dx = \frac{\sqrt{2\sqrt{d_y^4 + s} + 2d_y^2} \left(\sqrt{d_y^4 + s} - d_y^2\right)}{2\sqrt{d_y^4 + s}}. \quad (25)$$

Then, plugging (25) into (24), and substituting d_y by $d \sin(\theta_D)$ yields

$$\mathcal{L}_{I_X}(s) = \exp\left(-p\lambda_X \pi \mathcal{V}_x(s)\right), \quad (26)$$

where

$$\mathcal{V}_x(s) = \frac{\sqrt{2\sqrt{(d \sin(\theta_D))^4 + s} + 2(d \sin(\theta_D))^2}}{2\sqrt{(d \sin(\theta_D))^4 + s}} \times \sqrt{(d \sin(\theta_D))^4 + s - (d \sin(\theta_D))^2}. \quad (27)$$

Following the same steps above, and without details for the derivation, the Laplace transform expressions of the interference for an intersection scenario, when $\alpha = 4$ are given by

$$\mathcal{L}_{I_Y}(s) = \exp\left(-p\lambda_Y \pi \mathcal{V}_y(s)\right), \quad (28)$$

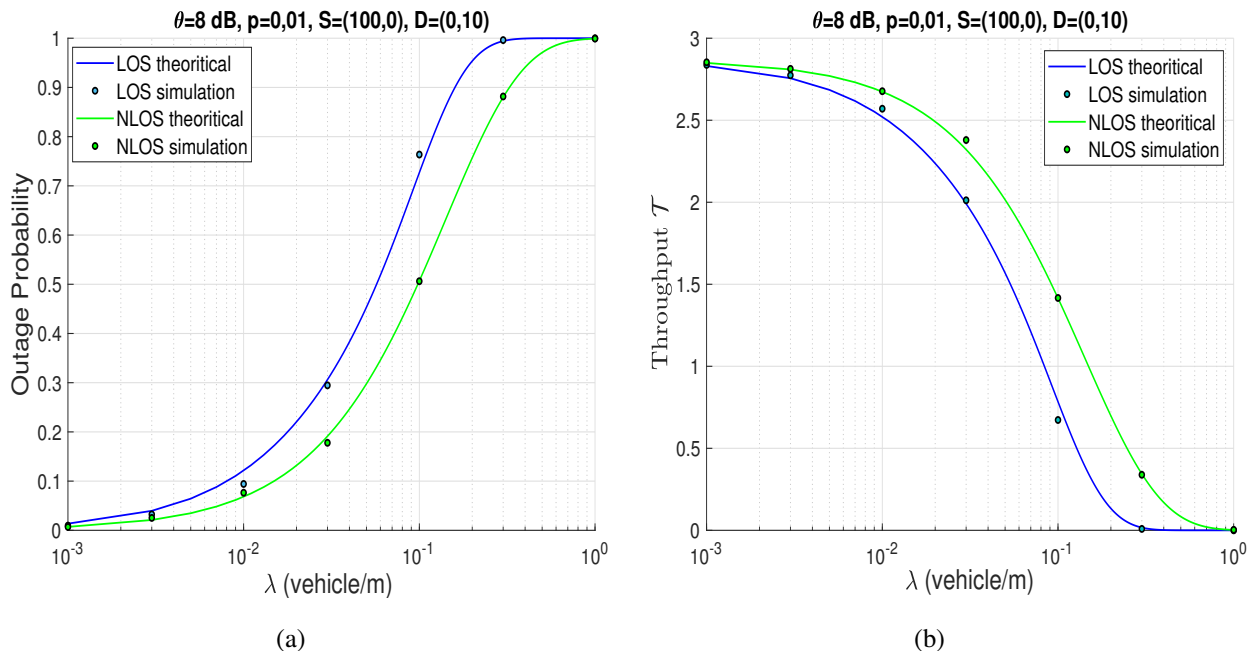


Fig. 2: Performance of VCs as a function of the vehicles density λ . (a) Outage probability for suburban environment (LOS), and urban environment (NLOS). (b) throughput for suburban environment (LOS), and urban environment (NLOS).

where

$$\mathcal{V}_y(s) = \frac{\sqrt{2\sqrt{(d \cos(\theta_D))^4 + s} + 2(d \cos(\theta_D))^2}}{2\sqrt{(d \cos(\theta_D))^4 + s}} \times \sqrt{(d \cos(\theta_D))^4 + s - (d \cos(\theta_D))^2}. \quad (29)$$

V. SIMULATIONS AND DISCUSSIONS

In this section, we evaluate the performance of a transmission between S and D at intersections. In order to verify the accuracy of the theoretical results, Monte Carlo simulations are obtained by averaging over 50,000 realizations of the PPPs and fading parameters. We set our simulation area to $[-10^3\text{m}, 10^3\text{m}]$ for each road. Without loss of generality, we set $\lambda_X = \lambda_Y = \lambda$. Finally, we consider $\alpha_{\text{LOS}} = 2$, $m_{\text{LOS}} = 3$, $\alpha_{\text{NLOS}} = 4$, $m_{\text{NLOS}} = 1$, and $\mu = 1$.

Fig.2 depicts the performance of VCs in terms of outage probability and throughput as a function of vehicles density for LOS and NLOS. We define the throughput, denoted \mathcal{T} as follows

$$\mathcal{T} = \mathbb{P}(\text{SIR} \geq \Theta) \times \log_2(1 + \Theta).$$

We see from Fig.2 that, as the vehicles intensity increases, the outage probability increases, and the throughput decreases. This is because, as intensity increases, the aggregate interference at the receiver increases as well. Hence, reducing the SIR, which will cause an increase in the outage probability, and a decrease in throughput. Surprisingly, we can see that, NLOS scenario has a better performance than LOS scenario, even though the fading degree of NLOS is higher than LOS ($m_{\text{LOS}} > m_{\text{NLOS}}$). This is due to the fact that, $\alpha_{\text{NLOS}} > \alpha_{\text{LOS}}$. Hence, the signals of interfering vehicles for NLOS scenario decrease rapidly compared to the signals of LOS scenario. Therefore, the aggregate of the interference in LOS scenario is greater than NLOS scenario. We can draw the conclusion that suburban intersections exhibit lower performance than urban intersections.

Fig.3 shows the performance of VCs transmission when S and D move towards the intersection. We notice that, when S and D move toward the intersection, the performance decrease. This is because at intersection, all the interfering vehicles interfere at D , which is not the case when D is far from the intersection. We also notice, as in Fig.2, that the LOS scenario has less performance than NLOS scenario. For instance, in Fig.3a, the throughput in NLOS scenario starts to decrease when D is at 400 m from the intersection, whereas the throughput in LOS scenario starts to decrease when D is at 1000 m from the intersection. For comparison purposes, we compared an intersection scenario with a highway scenario. We can see that the two scenarios offer the same performance when D is far from the intersection. However, a significant increase in outage probability can be noticed when D is at the intersection. For instance, the outage probability at intersection is 68% higher than in highway for LOS scenario.

Fig.4 shows the performance in terms of outage probability when the number of lanes increases. We can see that as the number of lanes increases, the outage probability increases accordingly. This is because, when the number of lanes increases, the number of interfering vehicles increases, which increases the interference at D , hence increasing the outage probability. We also see that the outage probability increases linearly with the number of lanes. Therefore, the gap in performance between LOS and NLOS scenario increases as the number of lanes increases.

VI. CONCLUSION

In this paper, we studied VCs at intersections, in the presence of interference over Nakagami- m fading channels. We derived the outage probability expressions for specific channel conditions, and when the nodes are either on the road or outside the road. We compared the performance

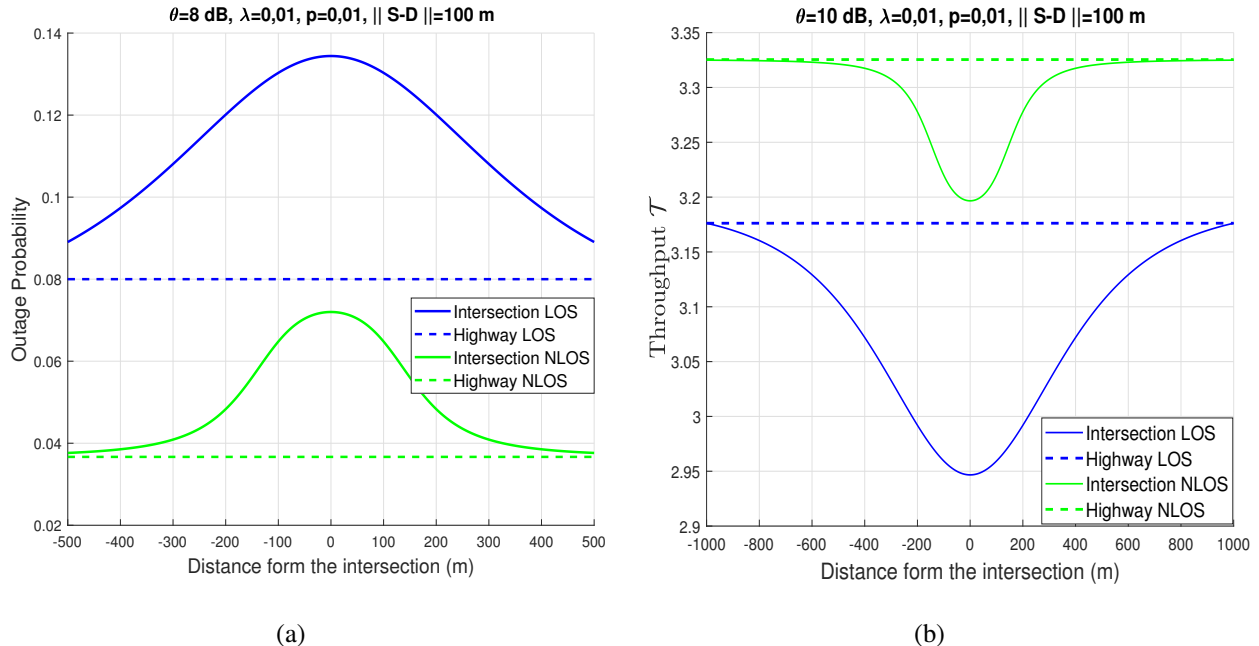


Fig. 3: Performance of VCs as a function of the distance between the transmitting nodes and the interaction. (a) Outage probability for suburban environment (LOS), and urban environment (NLOS). (b) throughput for suburban environment (LOS), and urban environment (NLOS).

of the suburban (LOS) environment and the urban (NLOS) environment, and showed that the urban environment exhibits better performance than the suburban environment. We also compared intersection scenarios with highway scenarios, and showed that the performance of intersection scenarios are worst than highway as the destination move toward the intersection. Finally, we investigated a realistic scenario involving many lanes, and showed that the increase of lanes decreases the performance.

REFERENCES

- [1] U.S. Dept. of Transportation, National Highway Traffic Safety Administration, “Traffic safety facts 2015,” Jan. 2017.
- [2] B. Blaszczyzyn, P. Muhlethaler, and Y. Toor, “Performance of mac protocols in linear vanets under different attenuation and fading conditions,” in *Intelligent Transportation Systems, 2009. ITSC’09. 12th International IEEE Conference on*, pp. 1–6, IEEE, 2009.
- [3] B. Blaszczyzyn, P. Muhlethaler, and Y. Toor, “Stochastic analysis of aloha in vehicular ad hoc networks,” *Annals of telecommunications-Annales des télécommunications*, vol. 68, no. 1-2, pp. 95–106, 2013.
- [4] B. Blaszczyzyn, P. Muhlethaler, and N. Achir, “Vehicular ad-hoc networks using slotted aloha: point-to-point, emergency and broadcast communications,” in *Wireless Days (WD), 2012 IFIP*, pp. 1–6, IEEE, 2012.

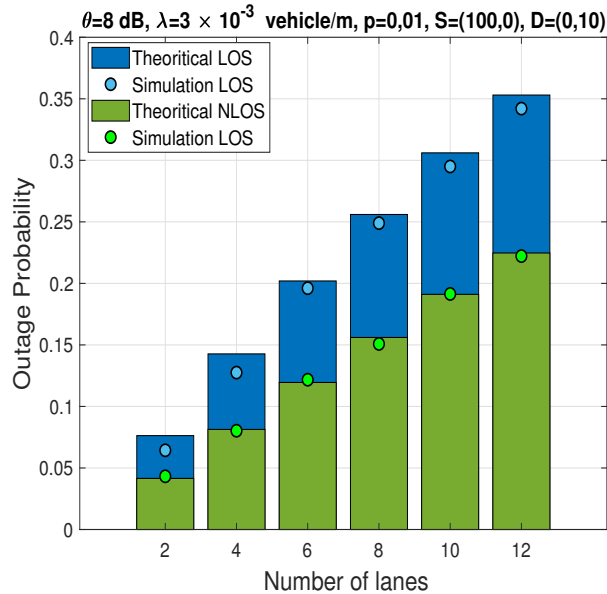


Fig. 4: Outage probability as a function of the number of lanes, for suburban environment (LOS), and urban environment (NLOS).

- [5] M. J. Farooq, H. ElSawy, and M.-S. Alouini, "A stochastic geometry model for multi-hop highway vehicular communication," *IEEE Transactions on Wireless Communications*, vol. 15, no. 3, pp. 2276–2291, 2016.
- [6] Z. Tong, H. Lu, M. Haenggi, and C. Poellabauer, "A stochastic geometry approach to the modeling of dsrc for vehicular safety communication," *IEEE Transactions on Intelligent Transportation Systems*, vol. 17, no. 5, pp. 1448–1458, 2016.
- [7] A. Tassi, M. Egan, R. J. Piechocki, and A. Nix, "Modeling and design of millimeter-wave networks for highway vehicular communication," *IEEE Transactions on Vehicular Technology*, vol. 66, no. 12, pp. 10676–10691, 2017.
- [8] A. Al-Hourani, R. J. Evans, S. Kandeepan, B. Moran, and H. Eltom, "Stochastic geometry methods for modeling automotive radar interference," *IEEE Transactions on Intelligent Transportation Systems*, vol. 19, no. 2, pp. 333–344, 2018.
- [9] E. Steinmetz, M. Wildemeersch, T. Q. Quek, and H. Wymeersch, "A stochastic geometry model for vehicular communication near intersections," in *Globecom Workshops (GC Wkshps), 2015 IEEE*, pp. 1–6, IEEE, 2015.
- [10] M. Abdulla, E. Steinmetz, and H. Wymeersch, "Vehicle-to-vehicle communications with urban intersection path loss models," in *Globecom Workshops (GC Wkshps), 2016 IEEE*, pp. 1–6, IEEE, 2016.
- [11] M. Abdulla and H. Wymeersch, "Fine-grained reliability for v2v communications around suburban and urban intersections," *arXiv preprint arXiv:1706.10011*, 2017.
- [12] J. P. Jeyaraj and M. Haenggi, "Reliability analysis of v2v communications on orthogonal street systems," in *GLOBECOM 2017-2017 IEEE Global Communications Conference*, pp. 1–6, IEEE, 2017.
- [13] T. Kimura and H. Saito, "Theoretical interference analysis of inter-vehicular communication at intersection with power control," *Computer Communications*, 2017.
- [14] B. E. Y. Belmekki, A. Hamza, and B. Escrig, "Outage performance of NOMA at road intersections using stochastic geometry," in *2019 IEEE Wireless Communications and Networking Conference (WCNC) (IEEE WCNC 2019)*, pp. 1–6, IEEE, 2019.
- [15] B. E. Y. Belmekki, A. Hamza, and B. Escrig, "On the performance of 5g non-orthogonal multiple access for vehicular

- communications at road intersections,” *Vehicular Communications*, p. doi:10.1016/j.vehcom.2019.100202, 2019.
- [16] B. E. Y. Belmekki, A. Hamza, and B. Escrig, “On the outage probability of cooperative 5g noma at intersections,” in *2019 IEEE 89th Vehicular Technology Conference (VTC2019-Spring)*, pp. 1–6, IEEE, 2019.
- [17] B. E. Y. Belmekki, A. Hamza, and B. Escrig, “Performance analysis of cooperative noma at intersections for vehicular communications in the presence of interference,” *Ad hoc Networks*, p. doi:10.1016/j.adhoc.2019.102036, 2019.
- [18] B. E. Y. Belmekki, A. Hamza, and B. Escrig, “Outage analysis of cooperative noma using maximum ratio combining at intersections,” in *2019 wireless and mobile computing, networking and communications (WiMob 2019), Barcelona, Spain*, pp. 1–6, 2019.
- [19] B. E. Y. Belmekki, A. Hamza, and B. Escrig, “Non-orthogonal multiple access performance for millimeter wave in vehicular communications,” *arXiv preprint arXiv:1909.12392*, 2019.
- [20] B. E. Y. Belmekki, A. Hamza, and B. Escrig, “Outage analysis of cooperative noma in millimeter wave vehicular network at intersections,” *arXiv preprint arXiv:1904.11022*, 2019.
- [21] B. E. Y. Belmekki, A. Hamza, and B. Escrig, “Performance analysis of cooperative communications at road intersections using stochastic geometry tools,” *arXiv preprint arXiv:1807.08532*, 2018.
- [22] B. E. Y. Belmekki, A. Hamza, and B. Escrig, “Cooperative vehicular communications at intersections over nakagami-m fading channels,” *Vehicular Communications*, p. doi:10.1016/j.vehcom.2019.100165, 07 2019.
- [23] S. Subramanian, M. Werner, S. Liu, J. Jose, R. Lupoie, and X. Wu, “Congestion control for vehicular safety: synchronous and asynchronous mac algorithms,” in *Proceedings of the ninth ACM international workshop on Vehicular inter-networking, systems, and applications*, pp. 63–72, ACM, 2012.
- [24] T. V. Nguyen, F. Baccelli, K. Zhu, S. Subramanian, and X. Wu, “A performance analysis of csma based broadcast protocol in vanets,” in *2013 Proceedings IEEE INFOCOM*, pp. 2805–2813, IEEE, 2013.
- [25] J. Hu, L.-L. Yang, and L. Hanzo, “Maximum average service rate and optimal queue scheduling of delay-constrained hybrid cognitive radio in nakagami fading channels,” *IEEE Transactions on Vehicular Technology*, vol. 62, no. 5, pp. 2220–2229, 2013.
- [26] L. Cheng, B. E. Henty, D. D. Stancil, F. Bai, and P. Mudalige, “Mobile vehicle-to-vehicle narrow-band channel measurement and characterization of the 5.9 ghz dedicated short range communication (dsrc) frequency band,” *IEEE Journal on Selected Areas in Communications*, vol. 25, no. 8, 2007.
- [27] M. Haenggi, *Stochastic geometry for wireless networks*. Cambridge University Press, 2012.